

A Pharmaceutical Cocrystal with Potential Anti-cancer Activity

Rajat Saha,^{a,†} Suman Sengupta,^{b,†} Sanjoy Kumar Dey,^{a, c†} Ian M. Steele,^d Arindam
Bhattacharyya,^{b,*} Susobhan Biswas,^{a,*} and Sanjay Kumar^{a,*}

^a*Department of Physics, Jadavpur University, Kolkata-700032, India, Email:*
susobhan1b@yahoo.co.in, Phone no: +91-9674028093 (S.B.), Email:
kumars@phys.jdvu.ac.in, Phone no: +91-9831115427 (S. K.).

^b*Department of Zoology, University of Calcutta, Kolkata-700060, India, Email:*
arindam19@yahoo.com, Phone no: +91-33-2461-5445 (A. B.)

^c*Department of physics, NITMAS, 24-Paragana(S)-743368, India*

^d*Department of the Geophysical Sciences, The University of Chicago, IL 60637, USA*

*Correspondence: Email: arindam19@yahoo.com, Phone no: +91-33-2461-5445 (A. B.);
Email: susobhan1b@yahoo.co.in, Phone no: +91-9674028093 (S. B.); Email:
kumars@phys.jdvu.ac.in, Phone no: +91-9831115427 (S. K.).

Additional title page Footnotes: R. S., S. S. and S. K. D have equal contributions.

General: Diacetyl monoxime, Thiosemicarbazide and Quinoxaline were purchased from Merck chemical company. All other chemicals used were of AR grade. Elemental analyses (CHN) were carried out using a Perkin-Elmer 240C elemental analyzer. IR studies were done on Nicolet Impact 410 spectrometer between 400 and 4000 cm^{-1} , using the KBr pellet method.

Crystallographic Data Collection and Refinement: Suitable single crystal of the cocrystal was mounted on a Bruker SMART diffractometer equipped with a graphite monochromator and Mo-K_α ($\lambda = 0.71073 \text{ \AA}$) radiation. The structure was solved using Direct method by using the SHELXS97. Subsequent difference Fourier synthesis and least-square refinement revealed the positions of the remaining non-hydrogen atoms. Non-hydrogen atoms were refined with independent anisotropic displacement parameters. Hydrogen atoms were placed in idealized positions and their displacement parameters were fixed to be 1.2 times larger than those of the attached non-hydrogen atom. Successful convergence was indicated by the maximum shift/error of 0.001 for the last cycle of the least squares refinement. All calculations were carried out using SHELXS 97 [1], SHELXL 97 [2], PLATON 99 [3], ORTEP-32 [4] and WinGX system Ver-1.64 [5]. Data collection and structure refinement parameters and crystallographic data for cocrystal were given in Table S2.

Reagents: DMEM medium with 4.0 mM L-glutamine, Antimycotic solutions, Gentamycin solution were purchased from HyClone, USA. Fetal calf serum was procured from HyClone. RNase A and sodium bicarbonate, were procured from Himedia chemicals. Propidium iodide and

DAPI were purchased from the sigma-Aldrich. NBT and BCIP were obtained from Himedia Chemicals. MTT was purchased from Chemi-Con International and H₂DCFDA was purchased from Millipore. PARP (#9532), Caspase 9 (#9508), GAPDH (#2118) antibodies were purchased from the Cell signaling Technology, Inc, USA and Bax (Sc-7480) was from Santa Cruz biotechnologies.

Phase contrast micrograph: Cells were seeded in a 6 well culture plate at a density of 5×10^4 cells/well and incubated in DMEM medium containing 10% FCS for 24 and 48 hr. After the adherent of cells, the cells were treated with the cocystal ranging from concentration (0-20 $\mu\text{g/ml}$) for 24 hr and one well kept as a control. After completion of treatment, the phase contrast micrograph was taken by Phase contrast microscope (Victory-FL “Dewinter-Italy”).

Nucleus staining by DAPI: For morphological examination of apoptotic changes, cells were stained with DAPI (Sigma Chemical Company St Louis, MO, USA). Human breast cancer (MCF-7) cells plated in a six-well culture plates (at a cell density 5×10^4 /well) were grown at 37° C for 24 h. The cells were exposed with the cocystal according to the respective dose for 24 h. After completion of the treatment, the cells were fixed for 15 min at room temperature in 4% paraformaldehyde and then washed with PBS. Fixed cells were incubated for 5 min at room temperature in dark with DAPI (1 mg/ml) and washed with PBS. Cells were examined by fluorescence microscopy (Victory-FL “Dewinter-Italy”). Apoptotic cells were identified by the condensation and fragmentation of their nuclei.

Immunoblotting: 90 mm Petri dishes were seeded with 9×10^6 cells and after washing in cold PBS, the cells were lysed using the lysis buffer (150 mM sodium chloride, 1.0% TritonX-100, 50 mM TRIS, pH 8.0, .01% SDS and 0.5% sodium deoxycholate) containing PMSF (1 mM),

aprotinin (1 µg/ml) and leupeptin (1 µg/ml). The supernatants were collected by centrifugation at 14000 rpm at 4°C for 15 min. The protein content was estimated using the Bradford method at 595 nm. Aliquots of 80 µg protein were loaded onto a 12.5% SDS-PAGE gel. The separated proteins were transferred onto a PVDF membrane (Millipore, Bedford, MA). The membrane was blocked in 5% non-fat dry milk and blotted with primary antibodies diluted in a blocking solution (5% BSA in TBS). After washing, the membrane was incubated with AP-conjugated secondary antibodies according to the manufacturer's instructions. Positive reactions were visualized using the developer NBT and BCIP solution. Western blot results were analyzed with a Bio-Rad Gel Documentation system.

Table S1: ^1H NMR data of the cocrystal, quinoxaline and TSBO

Compound	NH_2	$-\text{NH}-\text{N}$	CH_3	OH	quinoxaline ring	water
Cocrystal	7.7386, 8.3402	10.1868	2.48, 2.0665	11.550 2	3.3434, 8.9474, 8.0844-8.1171	3.3434
Quinoxaline					2.48635, 3.3999, 8.9438, 7.84701-8.11389	
TSBO	7.7297, 8.3290	11.5385	2.48 2.071	11.538 5		

Table S2: Crystallographic data collection and refinement parameters of cocrystal

Crystal Data	
Formula	C ₅ H ₁₀ N ₄ OS, C ₈ H ₆ N ₂ , H ₂ O
Formula Weight	322.40
Crystal System	Triclinic
Space group	P-1 (No. 2)
a [Å]	7.345(3)
b [Å]	8.053(3)
c [Å]	14.531(5)
α [°]	91.821(6)
β [°]	100.056(6)
γ [°]	115.273(5)
V [Å ³]	759.8(5)
Z	2
D(calc) [g/cm ³]	1.409
μ(MoKα) [/mm]	0.230
F(000)	340
Data Collection	
Temperature (K)	100
Radiation [Å]	MoKα 0.71073
θ Min-Max [°]	1.4, 28.4
Dataset	-9: 9 ; -10: 10 ; -19: 18
Tot. Data	9166
Uniq.	3635
R(int)	0.056
Observed data [I > 2.0 sigma(I)]	2468
Refinement	
Nref, Npar	3635, 201
R	0.0609
wR2	0.1548
S	0.95
Max. and Av. Shift/Error	0.00, 0.00
Min. and Max. Resd. Dens. [e/Å ³]	-0.41, 0.86

$$w = 1/[\sigma^2(F_o^2) + (0.0799P)^2] \quad \text{where } P = (F_o^2 + 2F_c^2)/3$$

Table S3: Hydrogen bonding dimensions of cocrystal

D-H...A	D-H/(Å)	H...A/(Å)	D...A/(Å)	< D-H...A/(°)	Symmetry
O1-H1...N5	0.84	2.12	2.956(3)	170	-1+x, y, z
O1W-H1W1...S1	1.11	2.37	3.447(3)	163	x, -1+y, -1+z
N1-H1A...O1W	0.88	2.28	3.032(3)	144	x, y, 1+z
N1-H1A...N3	0.88	2.31	2.664(3)	104	.
N1-H1B...N6	0.88	2.19	3.056(3)	166	x, y, 1+z
N2-H2...S1	0.88	2.87	3.557(3)	136	1-x, 2-y, 2-z
O1W-H2W1...O1W	1.05	2.16	2.819(4)	119	-x, -y, -z
C4-H4B...N4	0.98	2.40	2.750(3)	101	.
C5-H5A...O1	0.98	2.32	2.716(3)	103	.
C7-H7...N4	0.95	2.36	3.255(3)	157	1+x, y, z

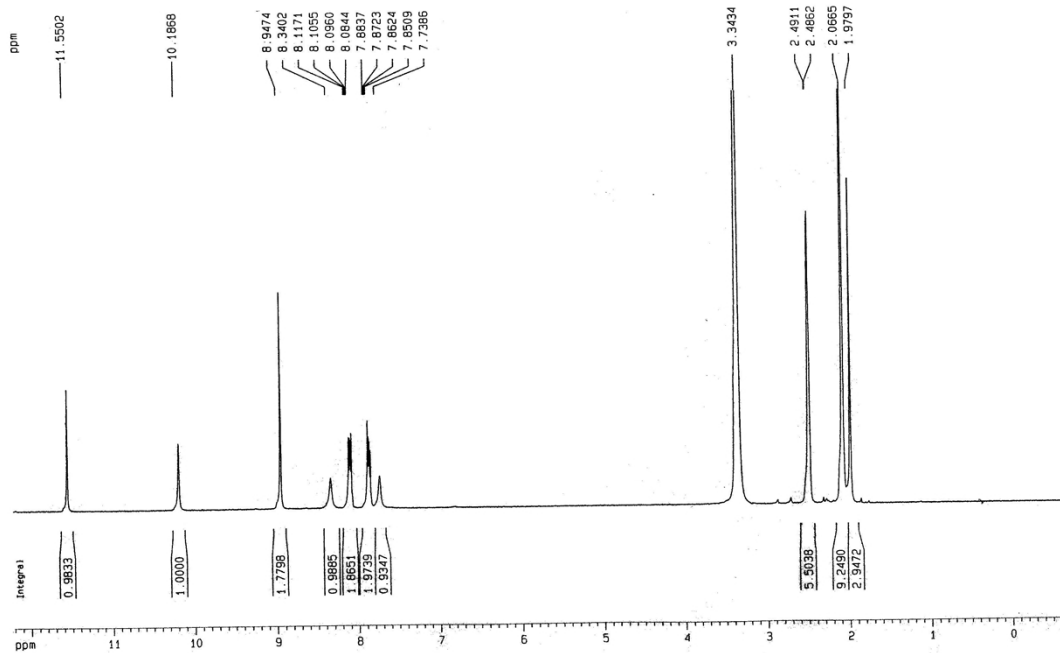


Fig. S1: ^1H NMR spectrum of the cocrystal.

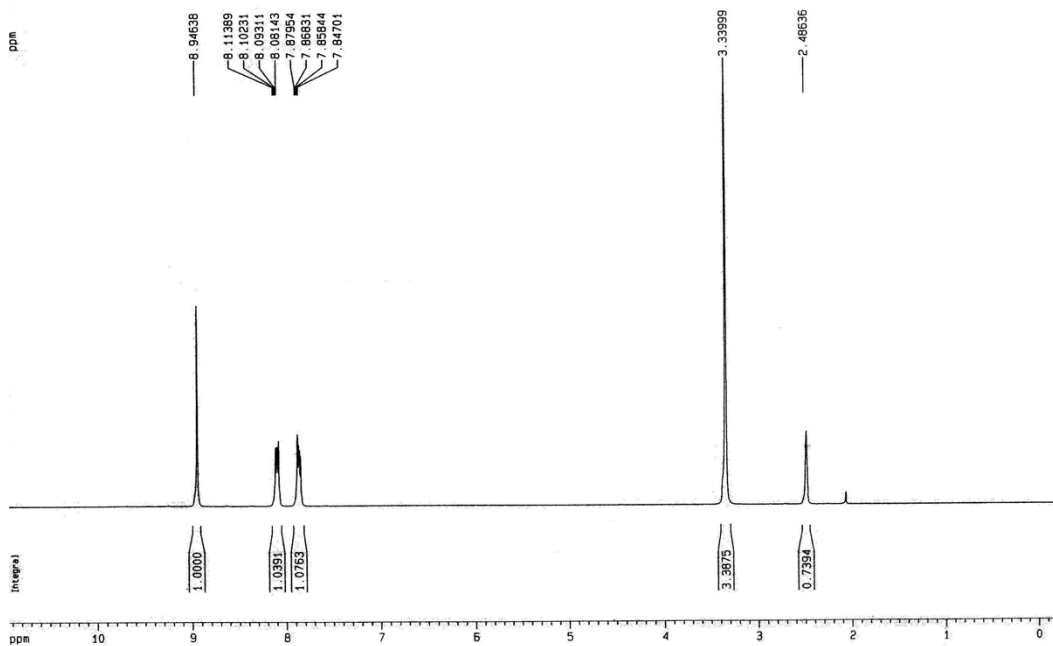


Fig. S2: ^1H NMR spectrum of quinoxaline.

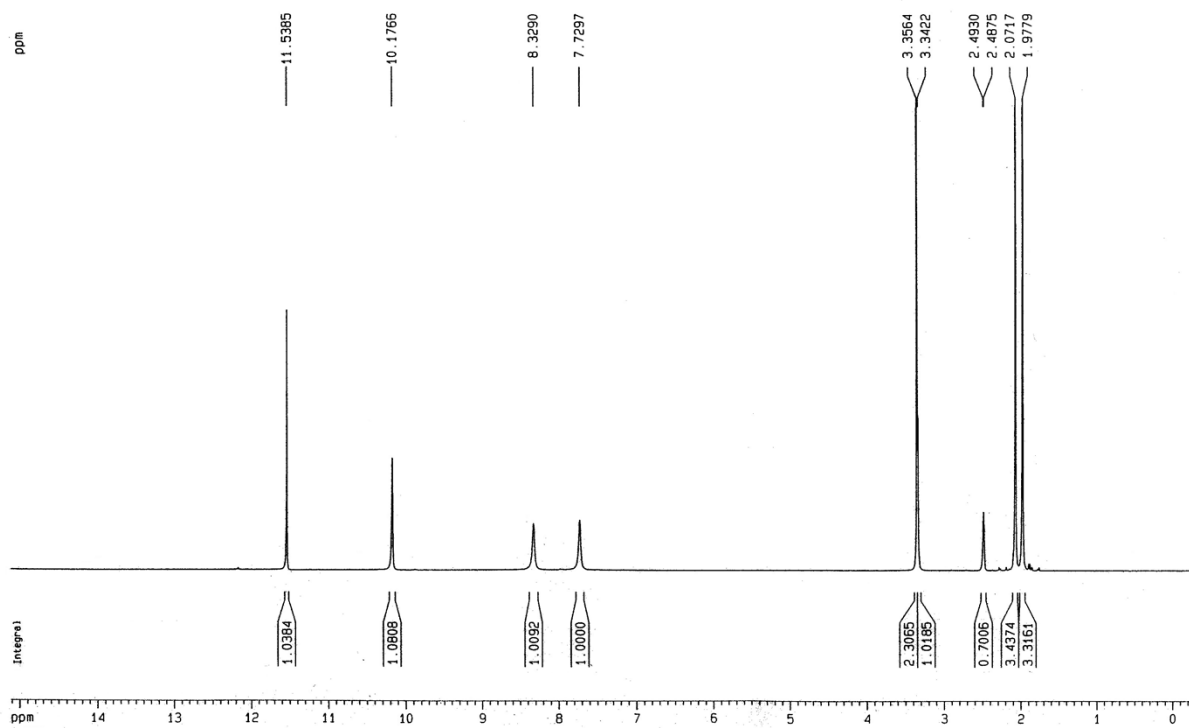


Fig. S3: ^1H NMR spectrum of TSBO.

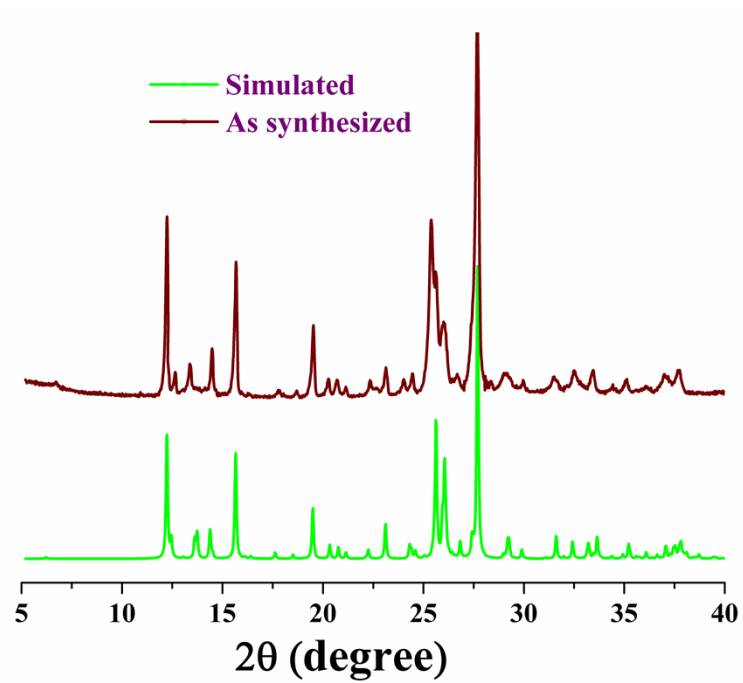


Fig. S4: PXRD pattern and simulated pattern of the cocrystal.

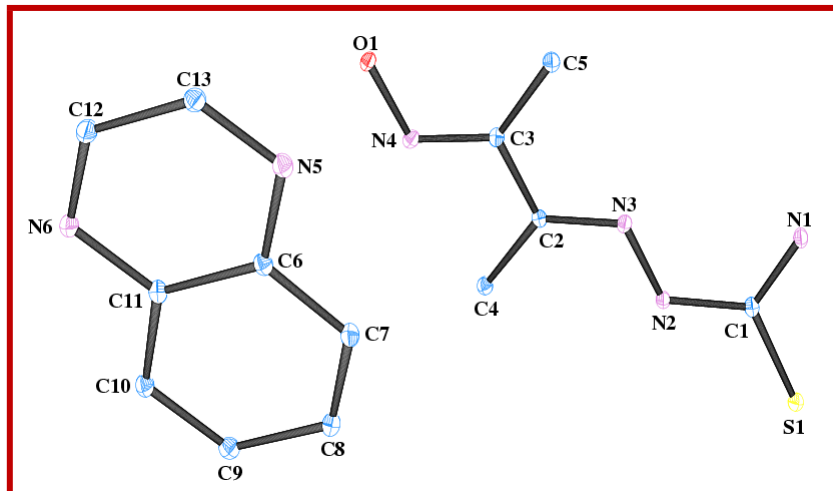


Fig. S5: ORTEP diagram of cocrystal.

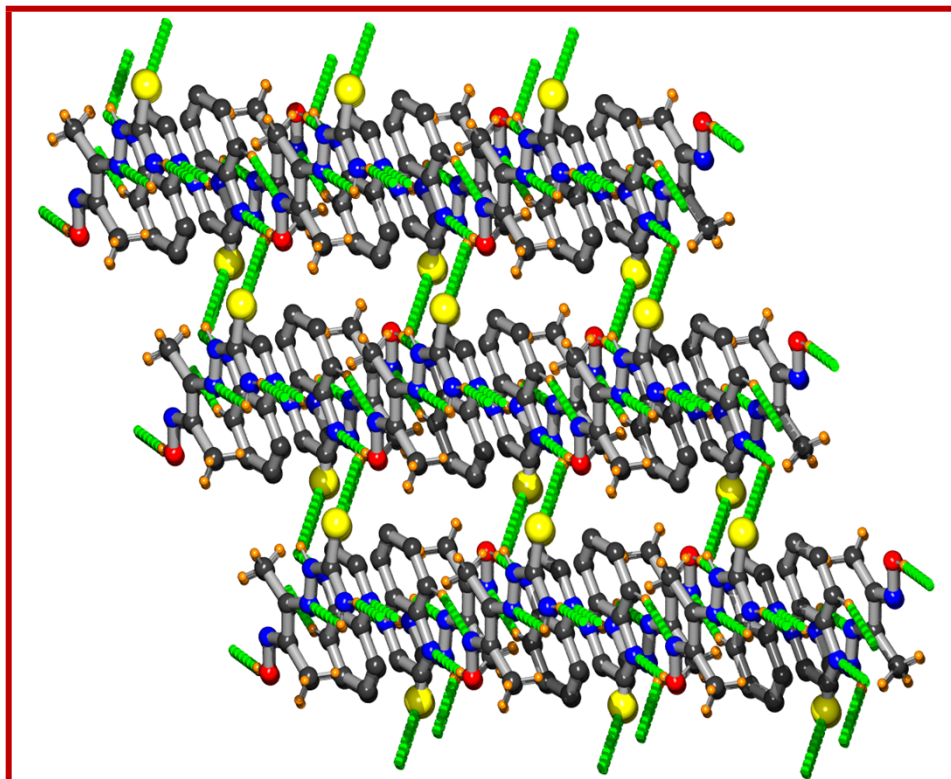


Fig. S6: 3D supramolecular structure formed by water mediated hydrogen bonding interaction

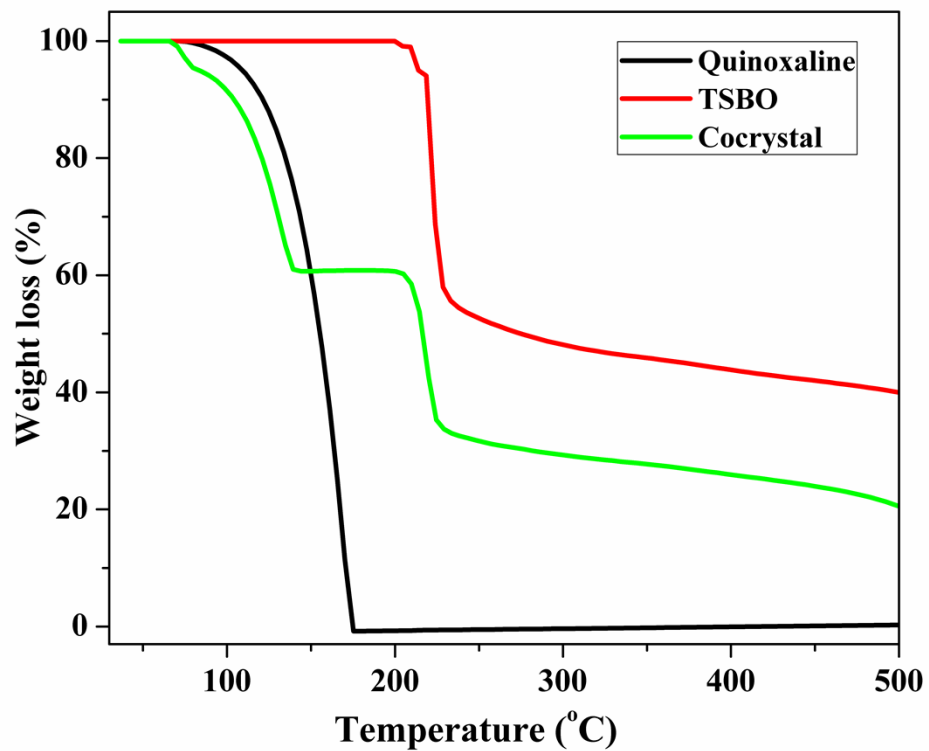


Fig. S7: TGA plots of quinoxaline, TSBO and the cocrystal

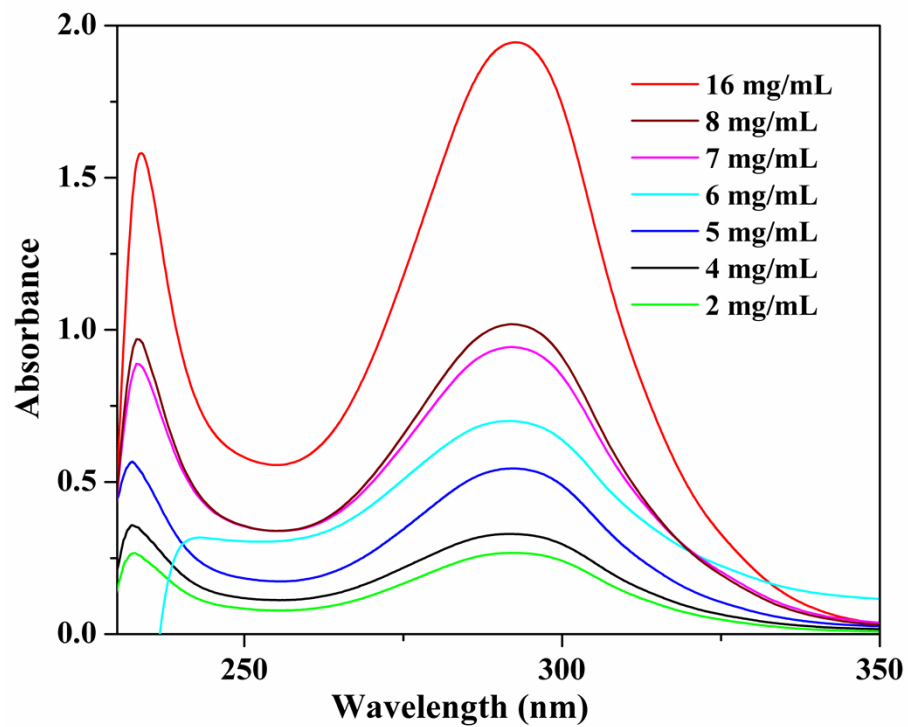


Fig. S8: The UV-vis absorbance curve of the cocrystal of different concentrations.

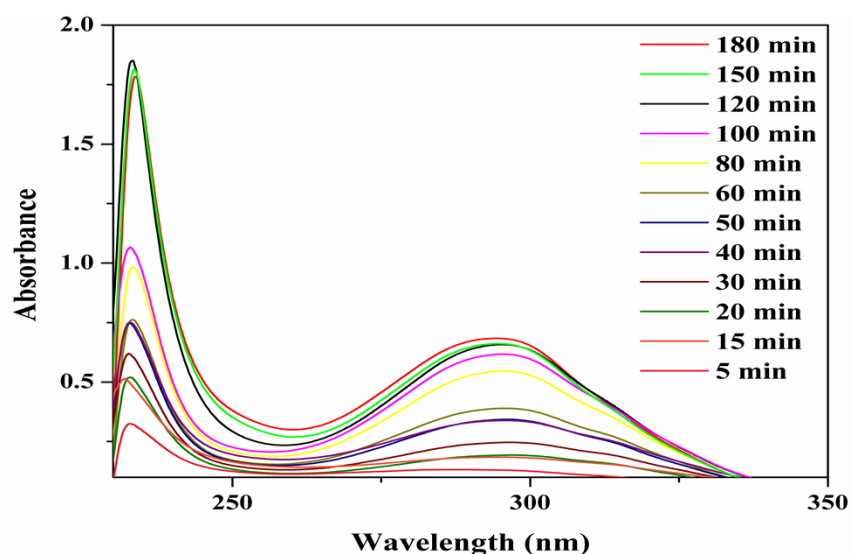


Fig. S9: The UV-vis absorbance spectra of the cocrystal solution collected at regular interval of time.

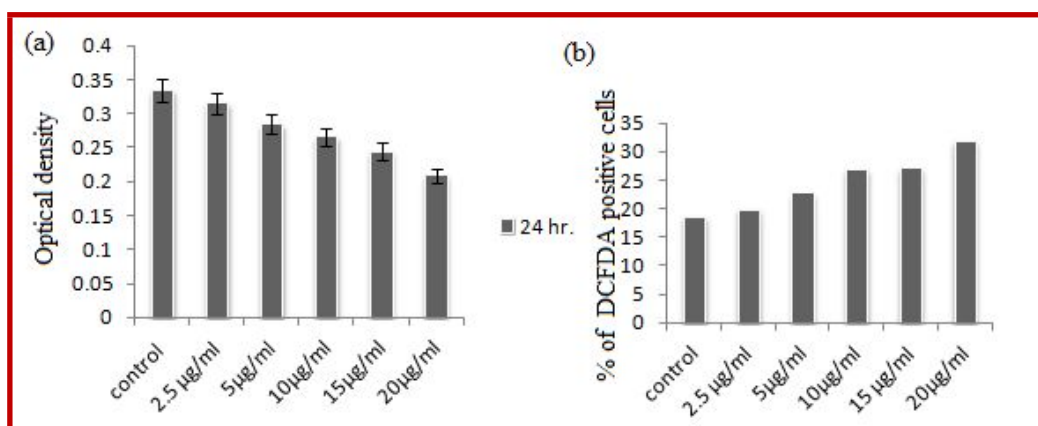


Fig. S10: Effect of cocrystal on A549 cells and ROS generation measurement. (a) A549 cells were incubated at a density of 5×10^3 cells/well in the presence of the cocrystal according to the respective concentration on 96-well plate for 24 h. MTT assay was done to determine change in proliferation. Data represent the mean \pm SE of three independent experiments. (b) A549 cells were incubated at a density of 5×10^4 cells/well in the presence of the cocrystal according to the respective concentration on 6-well plate for 24 h. ROS generation was measured by DCFDA on Flowcytometry. The bar graph represents the % of DCFDA positive cells vs. concentration.

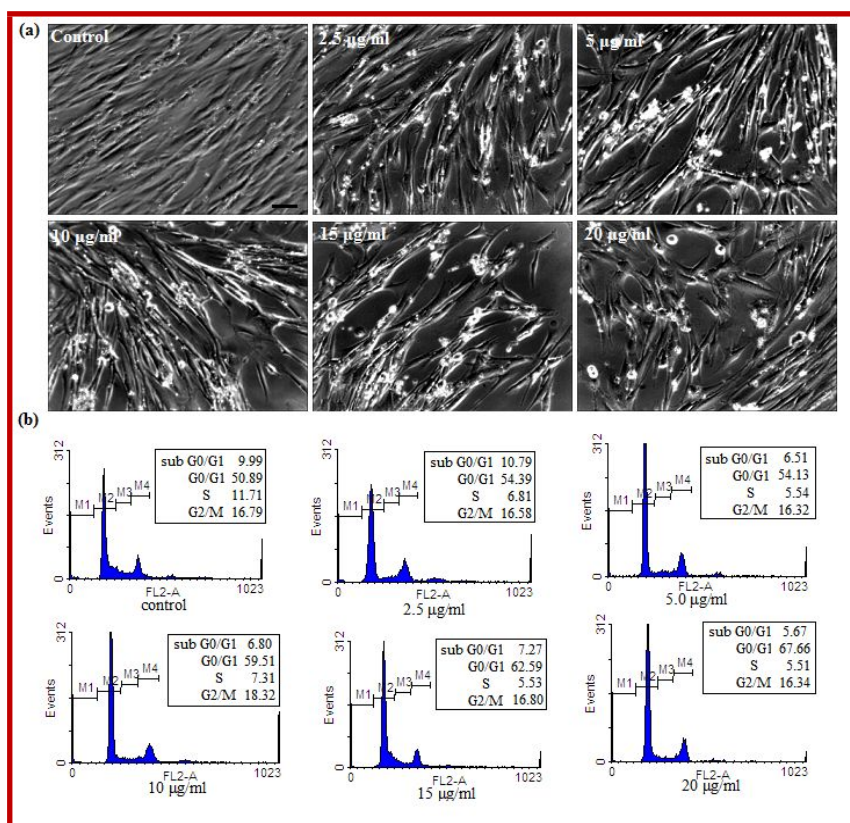


Fig. S11: The cocystal shows the growth inhibition to WI-38 cells. (a) Phase contrast micrograph (at 20X magnification) of WI-38 cells, after 24 h exposure of cocystal according to the respective conc. Scale bar =2 µm. (b) Flow cytometry analysis of cell cycle distribution pattern of WI-38 cells, after 24 h exposure of cocystal according to respective concentration. Histogram display represents PI fluorescence along X-axis (FL-2A) vs. events (along y-axis).

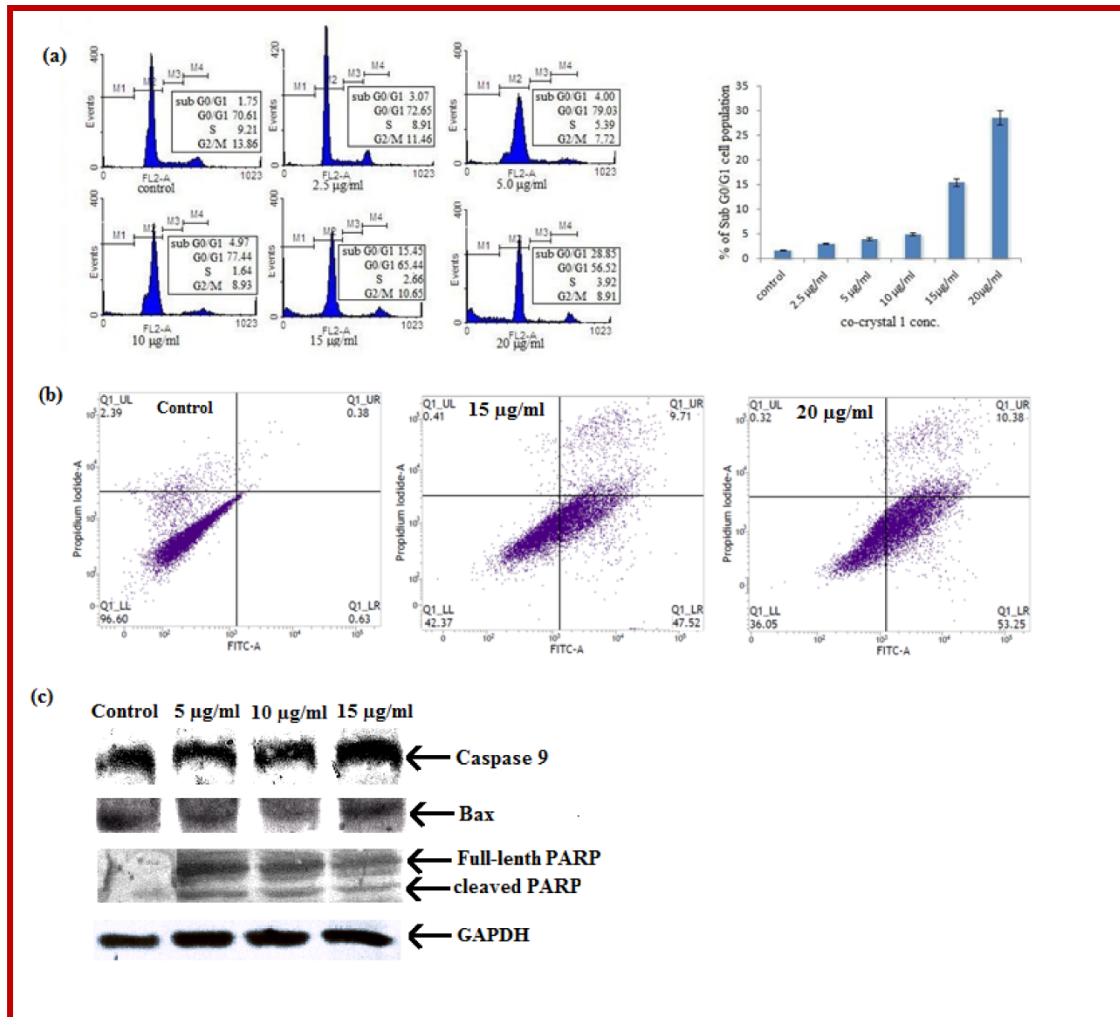


Fig. S12: Effect of the cocystal on cell cycle distribution of A549 cells; (a) Cell cycle distribution pattern of A549 cells by flowcytometry. Histogram display represents PI fluorescence along X-axis (FL-2A) vs. events (along y-axis). Bar graphs represent the % of subG0/G1 cell population with different concentration of the cocystal for 24 h exposure. The data represent the mean \pm SE of three independent experiments. (b) A fluorescence pattern of annexin V-propidium iodide (PI)-stained A549 cells after 24 h exposure of the cocystal according to the above concentration. (c) A549 cells were incubated with the cocystal according to the respective concentration for 24 h. The cell lysates were analyzed by immunoblotting with using PARP, caspase 9 and Bax antibodies. Here GAPDH used as a loading control.

References:

1. Sheldrick, G. M. SHELXS 97, Program for Structure Solution, University of Göttingen, Germany, **1997**.
2. Sheldrick, G. M. SHELXL 97, Program for Crystal Structure Refinement, University of Göttingen, Germany, **1997**.
3. Spek, A. L. *J. Appl. Crystallogr.* **2003**, *36*, 7–13.
4. Farrugia, L. J. *J. Appl. Crystallogr.* **1997**, *30*, 565–566.
5. Farrugia, L. J. *J. Appl. Crystallogr.* **1999**, *32*, 837–838.